Applied Catalysis B: Environmental 142–143 (2013) 647–653

Contents lists available at SciVerse ScienceDirect

Applied Catalysis B: Environmental

journal homepage: www.elsevier.com/locate/apcatb

Carbon nanotubes as an auxiliary catalyst in heterojunction photocatalysis for solar hydrogen

Gulzar Khan[a], Sung Kyu Choi[a], Soonhyun Kim[b], Sang Kyoo Lim[b], Jum Suk Jang[c], Hyunwoong Park[d,*]

[a] Department of Physics, Kyungpook National University, Daegu 702-701, Republic of Korea
[b] Division of Nano & Bio Technology, Daegu Gyeongbuk Institute of Science and Technology, Daegu 711-873, Republic of Korea
[c] Beamline Research Division, Pohang Accelerator Laboratory (PAL), POSTECH, Pohang 790-784, Republic of Korea
[d] School of Energy Engineering, Kyungpook National University, Daegu 702-701, Republic of Korea

ARTICLE INFO

Article history:
Received 26 February 2013
Received in revised form 27 May 2013
Accepted 31 May 2013
Available online 10 June 2013

Keywords:
Water splitting
Photodeposition
Artificial photosynthesis
Coupling
UV–vis absorption

ABSTRACT

This study demonstrates that multi-walled carbon nanotubes (CNTs) effectively catalyzes photocatalytic hydrogen production in heterojunction suspensions under solar visible light (AM 1.5G; $\lambda > 420$ nm). Due to the high catalytic activity of CNTs, use of Pt can be significantly reduced. For this, quaternary composites (CdS/TiO_2/Pt/CNTs) are prepared by the creation of CdS on platinized TiO_2 (TiO_2/Pt) subsequently to which chemically oxidized CNTs are loaded. A binary (CdS/TiO_2) and two ternaries (CdS/TiO_2/Pt and CdS/TiO_2/CNTs) are also prepared for comparison. A TEM analysis for the quaternary sample shows that TiO_2 is a central component that holds Pt nanoparticles, CNTs, and CdS clusters, while the last is spatially away from the catalysts. Photoluminescence (PL) emission bands of the binary excited at 325 nm and 410 nm are reduced by loading either Pt or CNTs, and further by co-loading of both catalysts. This suggests that the recombination of photogenerated charges under UV or visible light is inhibited due to cascaded charge transfer between TiO_2 and CdS, which is further decreased by Pt and/or CNTs. Photolysis confirms that either Pt or CNTs catalyzes effectively photocatalytic H_2 production in aqueous CdS/TiO_2 suspensions with sulfide/sulfite electron donor under visible light. Such activity is significantly enhanced by over 50% by co-loading of Pt and CNTs. It is found that the Pt amount can be reduced to approximately five- or one-tenth by additional loading of CNTs under an optimal condition. The maximized performance of the quaternary is also found in the significantly enhanced photocurrent generation compared to the two ternaries. The detailed mechanism and implications are discussed.

© 2013 Elsevier B.V. All rights reserved.

1. Introduction

Semiconductor photocatalysis-based solar hydrogen has received growing attention as an alternative to carbon-footprinted chemical fuels [1,2]. Its renewability and storability have great application potential to meet future global energy demands [2] as well as enable distributed power generation systems [3,4]. For high efficiency and low cost solar hydrogen, photocatalysts should absorb solar light abundantly, separate photogenerated charges efficiently, and catalyze hydrogen evolution effectively with reduced use of expensive materials [5]. Currently, a number of semiconductors are available as photocatalysts capable of producing hydrogen from water under normal sunlight or visible light. Among them, CdS may be the most ideal because of its narrow bandgap of max. 2.5 eV (corresponding to $\lambda <$ ca. 600 nm) and the suitable levels of the conduction band (CB: −0.75 V vs. NHE) and valence band (VB: 1.75 V vs. NHE). Although its photocorrosion still limits its widespread applicability, CdS is very useful as a model semiconductor for solar hydrogen.

CdS is often coupled to TiO_2 (hereafter CdS/TiO_2) to improve photocatalytic performance under ultraviolet + visible light or visible light only [6–11]. It was reported that the amount of H_2 produced in CdS/TiO_2 suspension is almost double of that in CdS under visible light ($\lambda > 420$ nm) [6]. A comparison of the photocurrent showed a similar degree of enhancement in the former. To further increase H_2 production, many catalysts are often deposited on CdS/TiO_2, among which platinum is by far the best. When Pt is located on the CdS surface ($Pt/CdS/TiO_2$), however, the Pt effect is very limited. For a maximal catalytic effect, Pt should be located on the TiO_2 surface (CdS/TiO_2/Pt) because most photogenerated electrons are effectively transferred to TiO_2 (Scheme 1) [6,12]. In comparison to $Pt/CdS/TiO_2$, H_2 production with ca. 40 times greater in CdS/TiO_2/Pt suspension shows the importance of the Pt location and particle-to-particle contact.

* Corresponding author. Tel.: +82 53 950 8973; fax: +82 53 950 8979.
E-mail address: hwp@knu.ac.kr (H. Park).

0926-3373/$ – see front matter © 2013 Elsevier B.V. All rights reserved.
http://dx.doi.org/10.1016/j.apcatb.2013.05.075

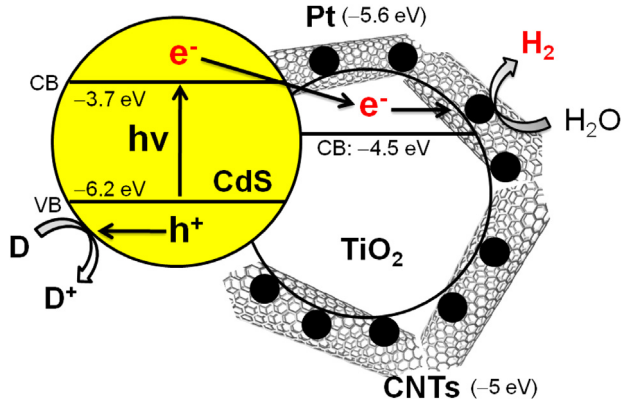

Scheme 1. Illustration of photogenerated charge transfers occurring in visible-light irradiated CdS/TiO_2/Pt/CNTs suspensions. CB, VB, and D refer to conduction band, valence band, and electron donor, respectively. Numbers are approximate work functions relative to vacuum levels. Under visible light ($\lambda > 420$ nm), photogenerated electrons are transferred from CdS to TiO_2 due to the wider work function (or lower CB position) of the latter. They continue to move forward interfacial CNTs and/or Pt because both are highly conductive. In this Scheme, Pt is illustrated as a final electron reservoir due to its wider work function (−5.6 eV) than CNTs (−5 eV). H_2 can be produced from CNTs as well, yet the amount may be smaller than that from Pt.

Recently, carbon materials have been employed for photocatalysis. When coupled to semiconductors (e.g., TiO_2 [13–15], CdS [16,17], CdSe [18,19]), the carbon materials enhance the photocatalytic activity primarily due to their unique physicochemical properties such as a large work function (4–5 eV), low electrical resistivity, high thermal conductivity, and large surface area [20,21]. For example, coupling of multi-walled carbon nanotubes (CNTs) to CdS (CdS/CNTs) enhances H_2 production by a factor of 17 under visible light [16]. Such an enhancement was attributed to the high electrical conductivity and catalytic surfaces of the CNTs. Although the surface area and the graphitic property (e.g., I_D/I_G) of the CNTs also influence H_2 production, a key factor may be the electrical conductivity [18]. Hence highly conductive graphites ($\sim 10^6$ S/m) are superior to CNTs with lower conductivity ($\sim 10^5$ S/m) in terms of H_2 production in visible light-irradiated CdSe suspensions [18].

In this study we examined the effects of CNTs on the photocatalytic H_2 production in CdS/TiO_2 composite suspensions under a simulated solar visible light ($\lambda > 420$ nm, AM 1.5G, 100 mW/cm^2). The primary aim is to address the following questions: (1) Can CNTs enhance the photocatalytic activity of the composites? (2) If so, can CNTs replace Pt as a hydrogen production catalyst? (3) If not, can CNTs be used as an auxiliary catalyst of Pt? For this, CNTs were chemically oxidized to increase the aqueous dispersibility, surface area, and electrical conductivity [18]. Then, the optimal amounts of CNTs and Pt on CdS/TiO_2 were determined in terms of H_2 production. Various surface analyses and photoelectrochemical studies were also performed to understand the effect and role of CNTs.

2. Experimental

2.1. Single materials

Multi-walled carbon nanotubes (CM-100, Hanwha Nanotech) were used as-received or after acid treatment. For the acid treatment, **CNTs** (1 g/L) were refluxed in aqueous nitric acid (1 M) for 1 h, filtered with 0.45-μm PTFE filters (Millipore), washed with a copious amount of distilled water, and subsequently dried overnight at 80 °C. When necessary, CNTs were annealed at 500 °C for 10 min. **TiO_2** (Degussa P25) was employed as a supporting material. It is a mixture of anatase and rutile (8:2) with a primary particle size of ca. 30 nm and has a BET surface area of ca. 50 m^2/g. **CdS** was prepared with a simple hydrolysis method [6,7,16]. A solution of sodium sulfide (Na_2S) was added dropwise to cadmium acetate solution ($Cd(CH_3COO)_2{\cdot}2H_2O$) with a molar ratio of 1:1, which was stirred for 1 h, filtered with 0.45-mm PTFE filters, washed with distilled water, and dried overnight at 80 °C.

2.2. Heterojunction materials

TiO_2/Pt was prepared by following a typical photodeposition method [22]. In brief, TiO_2 suspensions at 0.5 g/L with methanol (1 M) and various Pt(IV) ($H_2PtCl_6{\cdot}6H_2O$, Aldrich) concentrations (0.01 mM, 0.05 mM, and 0.1 mM) were irradiated with a 1.4-W UV lamp (Moolim, F8T5BLB) for 2 h, washed with distilled water, and collected as a dried powder. **TiO_2/CNTs** (or **TiO_2/Pt/CNTs**) composites were prepared with a hydration/dehydration method [13]. First, approximately 10 mg CNTs (virgin or acid-treated) were dispersed in water in a 200-mL beaker and sonicated for 20 min. Three different amounts of TiO_2 powder (or TiO_2/Pt) were added to the CNTs suspensions to make the relative amounts of CNTs be 1, 5, and 10 wt% during sonication. Then, the mixed suspensions were heated to 80 °C on a stir plate with air-flowing across the surface of the suspension to accelerate the evaporation of water. After evaporation, the composite was dried overnight in an oven at 104 °C to avoid any physicochemical change of the CNTs that occurs at higher temperatures in the presence of oxygen. **CdS/TiO_2**, **CdS/TiO_2/Pt**, **CdS/TiO_2/CNTs**, and **CdS/TiO_2/Pt/CNTs** were prepared by following the above CdS preparation method in aqueous suspensions of TiO_2, TiO_2/Pt, TiO_2/CNTs, and TiO_2/Pt/CNTs, respectively, at a weight ratio of 7:1 (CdS:TiO_2). For comparison, **(CdS/TiO_2)/CNTs** was also prepared by loading CNTs on as-prepared CdS/TiO_2 composites.

2.3. Photocatalytic and photoelectrochemical tests

Aqueous suspensions containing samples (0.5 g/L) and electron donors (0.1 M Na_2S and 0.1 M Na_2SO_3) were stirred in a Pyrex-glass reactor equipped with a quartz disc for light penetration. Prior to irradiation, nitrogen gas was purged through the suspension for 30 min, and the reactor was sealed from ambient air during the irradiation. A solar simulator equipped with AM 1.5G filter (LS-150 Xe, Abet Technologies) was used as a light source (100 mW/cm^2) with a cutoff filter ($\lambda > 420$ nm). To avoid thermal effects, the reactor was cooled to room temperature with an air cooler fan. During irradiation, the headspace gas of the reactor was intermittently sampled and analyzed for H_2 using a gas chromatograph (Young Lin, ACME 6100) equipped with a thermal conductivity detector and a carboxen 1000 packed column.

Photocurrents were collected on an inert working electrode (Pt wire) immersed in aqueous suspensions of photocatalysts (0.5 g/L, 0.95 M NaOH) using methyl viologen (MV^{2+}, 0.5 mM) as an electron shuttle described elsewhere [23]. A saturated calomel electrode (SCE) and a graphite rod were used as a reference and counter electrode, respectively. For the measurement of the MV^{2+}-mediated photocurrent, the working electrode was held at −0.4 V vs. SCE with a potentiostat/galvanostat (Versastat 3–400). Before and during irradiation, nitrogen gas was continuously purged through the suspensions, and a solar simulator with a cutoff filter ($\lambda > 420$ nm) was used as a light source (see Fig. 7 inset).

2.4. Surface analysis

UV–vis diffuse reflectance absorption spectra (DRS) were obtained by using a UV–vis spectrometer (UV-2450, Shimadzu). $BaSO_4$ was used as a reflectance standard. Transmission electron microscopy (TEM, Hitachi LTD, H-7600) was employed for examining the morphology of the samples. Photoluminescence spectra

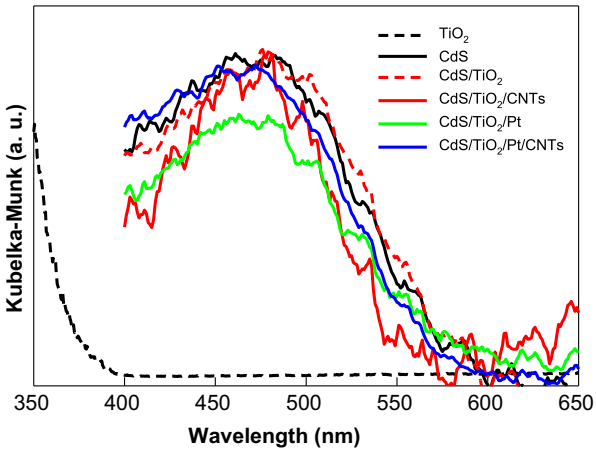

Fig. 1. UV–vis diffuse reflectance absorption spectra of composites. 0.4 wt% Pt and 5 wt% CNTs loaded.

were recorded at room temperature using a spectrometer (f = 0.5 m, Acton Research Co., Spectrograph 500i, U.S.A.) equipped with an intensified photodiode array detector (Princeton Instrument Co., IRY1024, U.S.A.). A He-Cd laser (Kimmon, 1K, Japan) with wavelengths of 325 nm and 410 nm and power of 50 mW was used as the excitation light source.

3. Results and discussion

3.1. Optical properties and surface analysis of the composites

The optical properties of the samples are very important because all photochemical processes are initiated by light absorption. Fig. 1 shows the UV–vis diffuse reflectance absorption spectra of the samples (expressed as a Kubelka–Munk unit). It is obvious that TiO_2 and CdS exhibit absorption edges at ca. 380 nm and 570 nm, corresponding to bandgaps of ca. 3.2 and 2.2 eV, respectively. A binary (CdS/TiO_2), two ternaries (CdS/TiO_2/Pt and CdS/TiO_2/CNTs), and a quaternary (CdS/TiO_2/Pt/CNTs) have similar absorption patterns to CdS. This indicates that the primary visible light ($\lambda > 420$ nm)-induced photoevents of the composites are critically influenced by CdS because TiO_2, Pt, and CNTs have virtually no absorption in the wavelength region. Among the various samples, CdS/TiO_2/Pt/CNTs was selected for a high resolution TEM analysis because this has the four components that are found in every combination of the samples (Fig. 2). It was found that the CdS clusters are located only on TiO_2 (Fig. 2a and b) while Pt nanoparticles of ~2 nm are also uniformly deposited only on TiO_2 (Fig. 2b and d). On the other hand, CNTs with a wall number of ~13 (inter-wall distance of ~0.2 nm) and inner diameter of ~6 nm (Fig. 2c) cross over TiO_2 particles. They can directly contact post-loaded CdS particles yet their primary contact is completed with TiO_2 and TiO_2/Pt (Fig. 2e and f) because TiO_2/CNTs (or TiO_2/Pt/CNTs) composites are prepared earlier. The post-loaded CdS particles are mostly found on TiO_2 likely due to the preferential interaction of the CdS precursors and TiO_2 surface and thereby their selective growth on TiO_2 [7]. These interparticle configurations are very important for cascaded charge transfer particularly in visible light-irradiated CdS/TiO_2 suspensions. As shown in Scheme 1, a comparison of the energy levels suggests that Pt and/or CNTs should be located at the TiO_2 side because of their wider work functions (Pt: −5.6 eV, CNTs: −5 eV) than that of CdS (−3.7 eV) and TiO_2 (−4.5 eV) [16,24], while CdS should directly contact TiO_2 for facile charge transfer. The loading of catalysts at the CdS side are less effective than that at the TiO_2 side because most of the photogenerated charge carriers will be preferentially transported to TiO_2 according to the potential gradient.

To examine photogenerated charge transfer pathways, photoluminescence (PL) emission spectra were obtained for the composites excited at wavelengths of 325 nm and 410 nm (Fig. 3). In general, PL emission energies are less than the bandgap energies because the emissions arise from the transitions of donor, acceptors, and surface traps [7,25–28]. In Fig. 3, excitation of CdS/TiO_2 at 325 nm generates two emission bands at around 495 nm and 650 nm irrespective of the composites. The former is very weak and could be attributed to the emissions from the conduction bands of TiO_2 and/or CdS to an acceptor level. Meanwhile, the latter is very strong and corresponds to ca. 1.91 eV. This emission appears to be associated with several transitions involving the donor–valence state, conduction–acceptor state, and/or donor–acceptor state, all of which are a kind of charge recombination [25–27]. An oxygen-coordinated Cd (e.g., CdO) often works as a donor while excess Cd serves as an acceptor [26]. Most important is the decrease of this emission as Pt or CNTs are loaded onto CdS/TiO_2, and such a decrease becomes more significant upon co-loading of Pt and CNTs (CdS/TiO_2/Pt/CNTs). This indicates that both catalysts are effective in inhibiting the charge recombination with a similar degree of effect, while the inhibition effect is more pronounced with the co-loading of Pt and CNTs. It is presumed that photogenerated electrons are effectively transported from CdS/TiO_2 to the catalysts through TiO_2 (cascaded charge transfer) while holes have counter flows (from TiO_2 to CdS). To confirm this charge (particularly electron) transfer pathway, CdS is selectively excited at 410 nm (Fig. 3). Under this condition, no charge carriers are generated from TiO_2. A single emission band is obtained at 553 nm, nearly matching the absorption edge of CdS (Fig. 1). Hence this emission is attributed to a band–band transition or a band–shallow trap transition. Similar to the case of excitation at 325 nm, the emission is also decreased by the loading of Pt and/or CNTs. This is convincing evidence for the cascaded charge transfer.

3.2. Photocatalytic H_2 production

Fig. 4 shows the time-profiled H_2 production in bare CdS and CdS composite suspensions with a sulfide/sulfite mixture (each 0.1 M) as a hole scavenger under solar visible light ($\lambda > 420$ nm of AM 1.5G). Bare CdS, CdS/TiO_2, and CdS/CNTs exhibit similar activities with ca. 1 μmol-H_2/h (Fig. 4 inset) although the last two may have enhanced charge separation and catalytic property, respectively. This indicates that (1) the enhanced charge separation at CdS/TiO_2 is not a critical factor for H_2 production in the absence of a catalyst and (2) the effect of the CNTs on the H_2 production by bare CdS is insignificant because of the rapid charge recombination. Therefore, to enhance charge separation and catalyze H_2 production, a ternary junction of CdS, TiO_2, and CNTs should be constructed. Two different ternary composites were compared: CdS/TiO_2/CNTs vs. (CdS/TiO_2)/CNTs. The former was prepared by loading of CdS onto TiO_2/CNTs whereas the latter was obtained by loading of CNTs onto CdS/TiO_2 under exactly the same conditions. Nevertheless, the former exhibits over 10-fold larger H_2 production (ca. 26 μmol-H_2/h) compared to the latter (~2.6 μmol-H_2/h). It is of note that even the activity of the latter is around double of the aforementioned two binaries (CdS/TiO_2 and CdS/CNTs), indicating the superiority of the ternary structure and the cascaded charge transfer from CdS, TiO_2, and to CNTs. More important is the preparation order of the ternary determines the overall photocatalytic activity. When CdS and TiO_2 are coupled earlier, the post-loaded CNTs will have contact to not only TiO_2 but also CdS. This may diminish the catalytic effect of the CNTs because most of the photogenerated electrons are transported to TiO_2 and the fraction of CNTs at the CdS side is less functional (cf. CdS/CNTs). Conversely, post-loaded CdS is preferentially located on the TiO_2 side when TiO_2 is coupled to CNTs earlier (Fig. 2), making the CNTs more available for H_2 production.

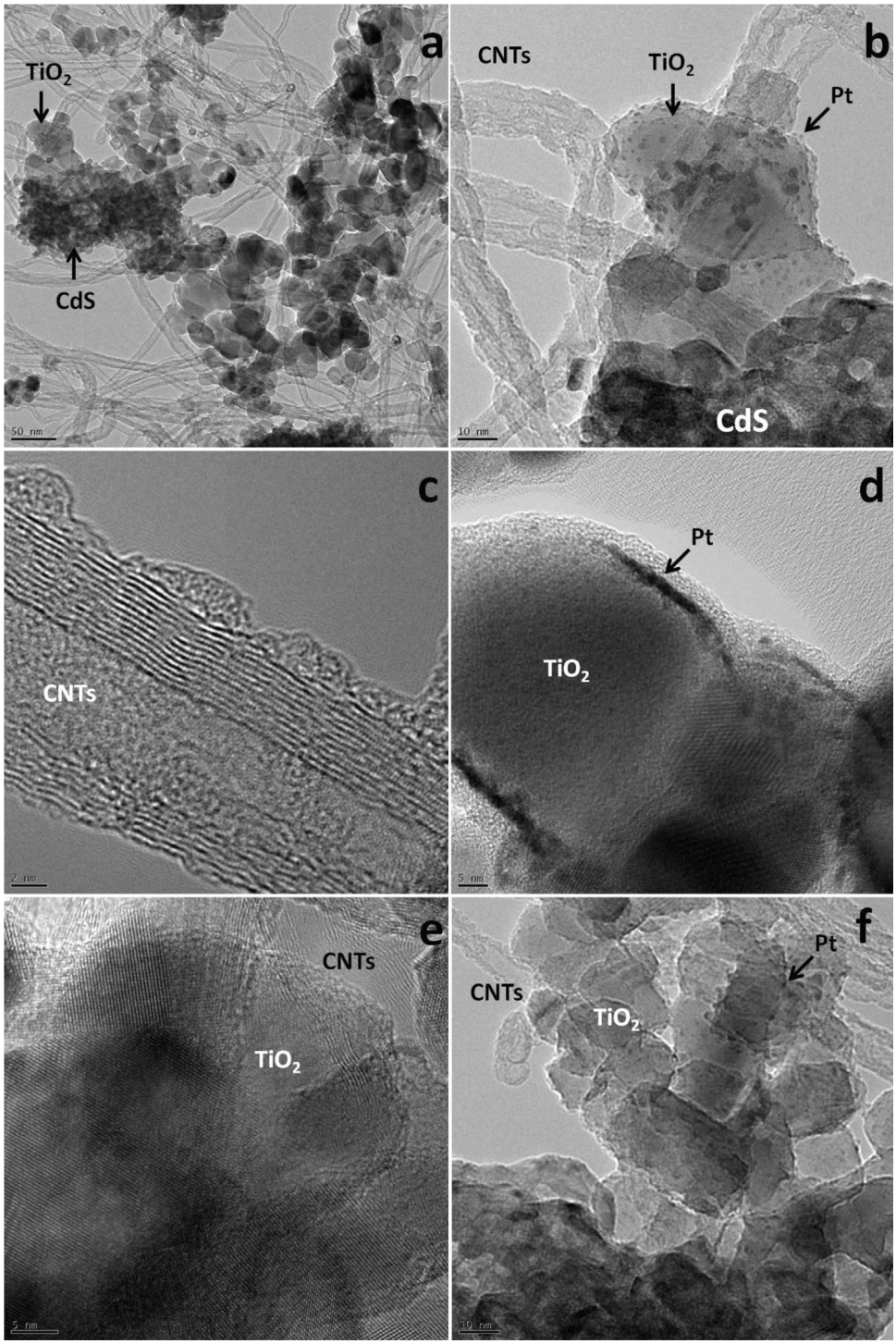

Fig. 2. High-resolution TEM images of CdS/TiO_2/Pt/CNTs composites. 0.4 wt% Pt and 5 wt% CNTs loaded.

The catalytic effect of CNTs was compared to that of Pt in terms of H_2 production as well. For this, three different amounts of Pt (0.4, 2, and 4 wt%) were deposited on TiO_2 (TiO_2/Pt), subsequently to which CdS was coupled (CdS/TiO_2/Pt). As expected, even a tiny amount of Pt (0.4 wt%) is very effective in catalyzing H_2 production (~40 μmol/h) in CdS/TiO_2 suspensions (Fig. 5). Large amounts of Pt loading enhance H_2 production (~70 μmol/h) but with less pronounced effect at 4 wt%, indicating the existence of an optimal Pt wt%. The negative effect at 4 wt% can be attributed to a light-screening and/or an active site-blocking effect of Pt. The former is often raised in the literature [5] but may be minor in this study because the surface coverage by Pt is insignificant (Fig. 2). It should be noted that Pt deposition occurs through the reduction of Pt(IV) to Pt(0) by the photogenerated electrons of TiO_2. The location of the Pt deposit is the photoactive site where electrons are created and transported. An increase in the deposited Pt nanoparticles therefore decreases the number of photoactive sites. To reduce the Pt amount and simultaneously increase the photocatalytic activity, CNTs (5 wt%) were loaded onto CdS/TiO_2/Pt (0.4 wt%). As shown in Fig. 5, the photocatalytic activity of the ternary with 0.4 wt% Pt is enhanced from ca. 40 to 60 μmol/h by the loading of CNTs. This activity is similar to those of the ternaries with 2 wt% and

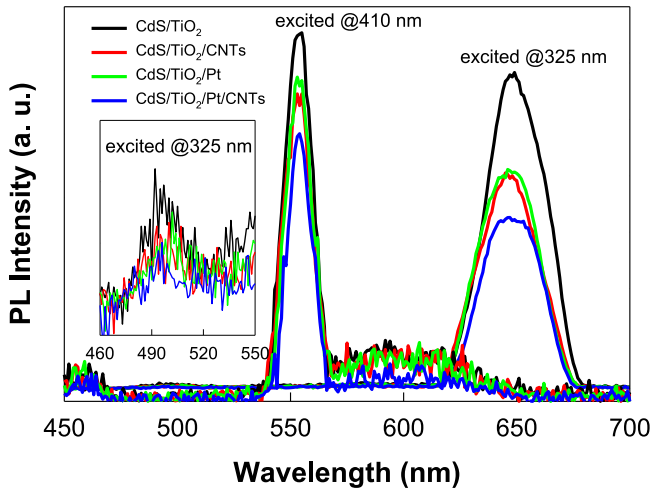

Fig. 3. Photoluminescence emission spectra of composites excited at 325 nm and 410 nm. Inset: magnified spectra (excited at 325 nm). 0.4 wt% Pt and 5 wt% CNTs loaded.

4 wt% Pt (Fig. 5b), which shows that the use of expensive Pt can be substantially reduced by the use of cheap CNTs.

Such a synergistic effect of the simultaneous loading of Pt (0.4 wt%) and CNTs is also confirmed by changing the CNTs amounts (Fig. 6a). It is obvious that even 1 wt% CNTs enhances H_2 production in the CdS/TiO_2/Pt suspension by 25%. Loading of 10 wt% CNTs also induces a positive yet less pronounced effect compared to 5 wt% CNTs presumably due to the light-screening effect of the CNTs with a high volume-to-mass ratio. This optimal CNTs content is changed when the pre-loaded Pt amount increases to 2 wt% (Fig. 6b). Under this Pt content, loading of CNTs enhances H_2 production with a maximal increase of 60% at 1 wt% CNTs (ca. 350 μmol in 3 h). Graphite oxides also induced synergistic H_2 production under UV when they are co-loaded with Pt on TiO_2 [29]. CNTs appear to play a similar role as graphite oxides even in ternary photocatalyst systems under visible light. Indeed, CNTs have already been reported as an effective electrocatalyst in dye-sensitized solar cells [30,31] and photocatalysis [13,16,18]. However, the synergistic effect of CNTs on the visible light-induced H_2 production in CdS/TiO_2/Pt system has not been reported yet.

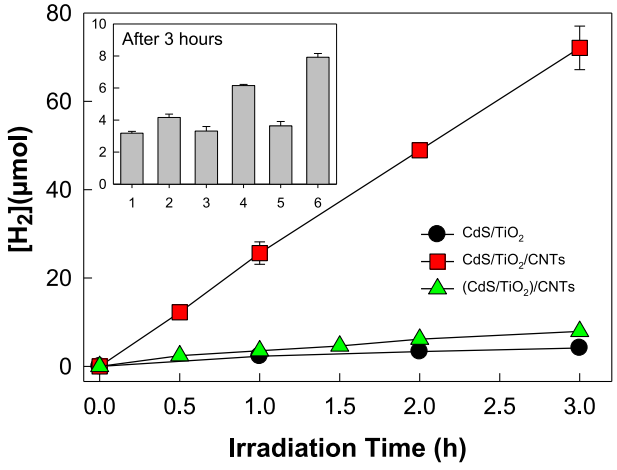

Fig. 4. Time-profiled H_2 productions in CdS/TiO_2 composite suspensions under solar visible light (AM 1.5G; 100 mW/cm^2; λ > 420 nm). [Photocatalyst] = 0.5 g/L; $[Na_2S]_0 = [Na_2SO_3]_0 = 0.1$ M. Inset: H_2 amounts produced in 3 h in the suspensions of CdS (1), CdS/TiO_2 (2), CdS/CNTs (3), CdS/TiO_2/CNTs (4: CNTs annealed at 500 °C for 10 min), CdS/TiO_2/CNTs (5: annealed at 500 °C for 10 min), and TiO_2/CdS/CNTs (6). For more detailed information on the samples, see Section 2.

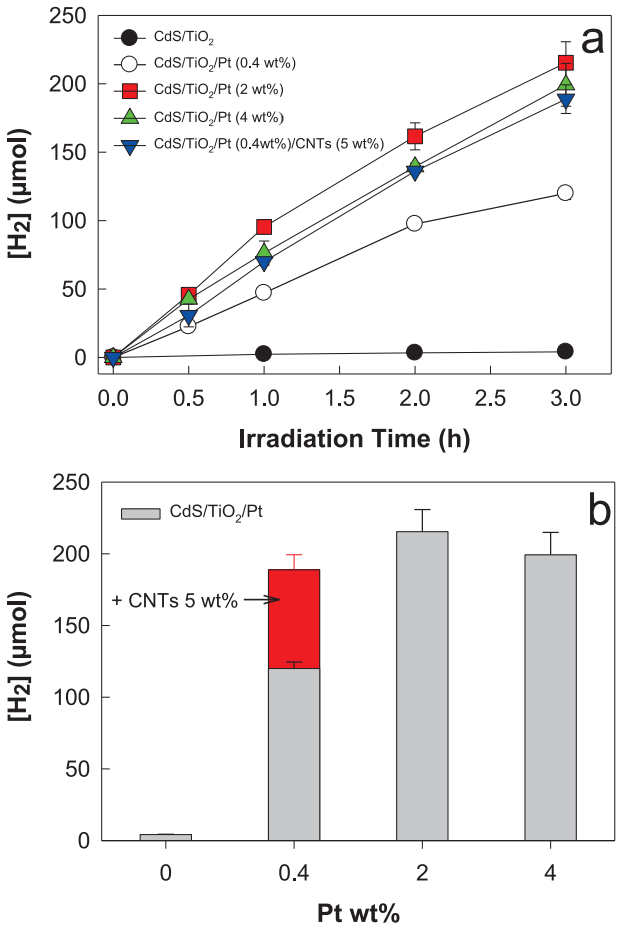

Fig. 5. (a) Time-profiled H_2 productions and (b) H_2 amounts produced (in 3 h) in CdS/TiO_2 composite suspensions under solar visible light (AM 1.5G; λ > 420 nm). [Photocatalyst] = 0.5 g/L; $[Na_2S]_0 = [Na_2SO_3]_0 = 0.1$ M.

3.3. Photocurrent generation

To compare the effects of CNTs on charge separation and catalysis (charge injection), photogenerated electrons are collected in photocatalyst suspensions under solar visible light (Fig. 7). Methyl viologen redox couple (E^0 (MV^{2+}/MV^+) = −0.44 V) was used as an electron shuttle between semiconductor particles and the collector electrode (Pt wire). No specific hole scavenger was added because (1) CdS could produce O_2 from water in the presence of an electron scavenger and (2) photogenerated electrons are efficiently trapped by MV^{2+} in a highly alkaline solution (pH ~13) due to the negative shifts of Fermi levels of CdS and TiO_2 (ca. −1.33 [32] and −0.87 V [23], respectively). All photocurrent (I) profiles show an exponential rise-to-maximum trend. The concentration of MV^+ (C_R) follows the same trend because of the correlation between I and C_R ($I = nF\delta \times C_R$, where δ is a constant) [33]. The profiles are classified into large (~28 μA) and small (~18 μA) current generation groups. The former includes CdS/TiO_2 and CdS/TiO_2/Pt/CNTs while the latter includes the other samples. Compared to CdS, a large current generation in CdS/TiO_2 is attributed to the enhanced charge separation. It is rather surprising that the deposit of Pt or loading of CNTs onto this CdS/TiO_2 decreases the current generation although they enhance significantly the photocatalytic H_2 production. More interesting is that the co-loading of Pt and CNTs increases the current generation to the level of CdS/TiO_2.

To understand these phenomena in terms of H_2 production, it should be noted that the MV^{2+}-induced current is generated via single-electron transfer ($MV^{2+} + e^- \rightarrow MV^+$) whereas H_2

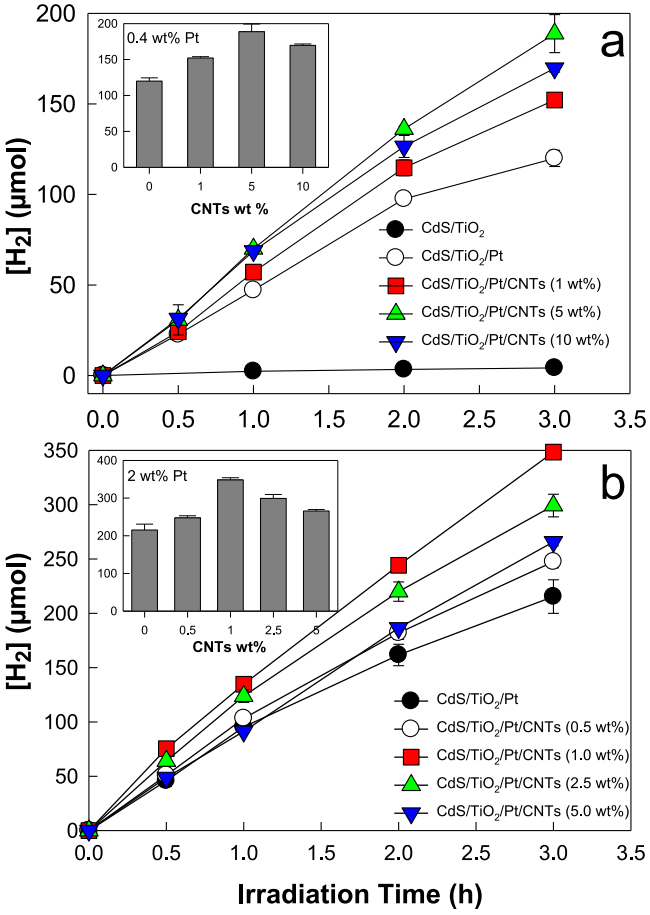

Fig. 6. Effects of CNT wt% on photocatalytic H_2 production in CdS/TiO_2/Pt composite suspensions with Pt of (a) 0.4 wt% and (b) 2 wt% under solar visible light (AM 1.5G; $\lambda > 420$ nm). [Photocatalyst] = 0.5 g/L; $[Na_2S]_0 = [Na_2SO_3]_0 = 0.1$ M. Insets: H_2 amounts produced in 3 h under the same experimental condition.

is produced via two-electron transfer ($2H_2O + 2e^- \rightarrow H_2 + 2OH^-$) through two consecutive steps (hydrogen adsorption and desorption) [34]. Hence the latter requires catalysts for effective multi-charge transfer whereas the former proceeds relatively efficiently without catalysts (e.g., CdS/TiO_2). The reduced current

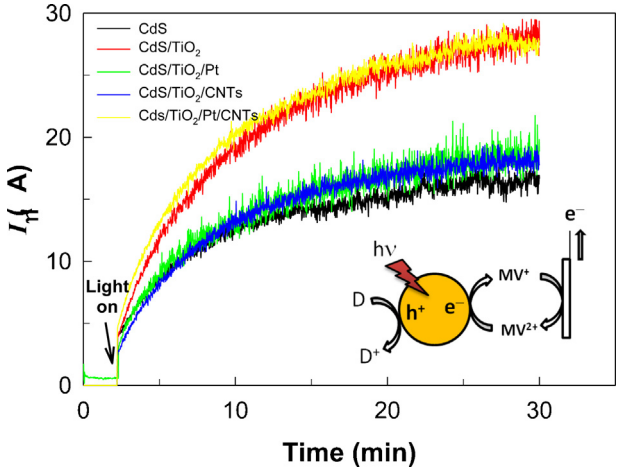

Fig. 7. Time-profiled photocurrent generation in various photocatalyst suspensions under solar visible light (AM 1.5G; $\lambda > 420$ nm). 0.4 wt% Pt and 5 wt% CNTs loaded; [Photocatalyst] = 0.5 g/L; $[MV^{2+}]_0 = 0.5$ mM; [NaOH] = 0.95 M; N_2 purged continuously through the suspensions; working electrode (Pt wire) held at −0.4 V vs. SCE. Inset: schematic illustration of this system.

generation in the two ternaries (CdS/TiO_2/Pt and CdS/TiO_2/CNTs) therefore indicates that single Pt nanoparticles or single CNTs are not effective in catalyzing single-electron transfer despite their effectiveness for multi-electron transfer. However the quaternary (CdS/TiO_2/Pt/CNTs) is very effective in catalyzing not only multi-electron transfer but also single electron transfer. It is uncertain how the quaternary exhibits such behavior, requiring further study. Nevertheless, the quaternary could be an ideal photocatalyst in terms of single and multi-electron transfer under visible light.

4. Conclusions

Although CNTs are widely used as a support of platinum in diverse fields, little evidence has been suggested for their synergistic effect on solar hydrogen production in heterogeneous photocatalytic systems. In this regard, the present study shows important evidence that photocatalytic H_2 production can be maintained even with reduced use of Pt by the loading of CNTs. This maintained activity results from the invariable catalysis of CNTs between CdS/TiO_2/CNTs and CdS/TiO_2/Pt/CNTs, suggesting that CNTs can be used as an auxiliary catalyst of Pt. In addition, this study demonstrates that how the hybrid is organized to facilitate the charge transfer. A comparison of the energy levels suggests that Pt and/or CNTs should be located at the TiO_2 side because of their wider work functions than that of CdS and TiO_2, while CdS should directly contact TiO_2 for facile charge transfer. The loading of catalysts onto CdS is less effective than that on TiO_2 because most of the photogenerated charge carriers will be preferentially transported to the latter according to the energy level. A variety of optimization-based approaches show that the quaternary should be an ideal photocatalyst in terms of single and multi-electron transfer under solar visible light.

Acknowledgments

This research was supported by the Basic Science Research Programs (Nos. 2012R1A2A2A01004517 and 2011-0021148) and the Korea Center for Artificial Photosynthesis (KCAP) (2012M1A2A2671779) through the National Research Foundation (NRF) funded by MEST, Korea.

References

[1] R. van de Krol, M. Gratzel, Photoelectrochemical hydrogen production, Springer, New York, 2012.
[2] A.J. Bard, M.A. Fox, Accounts Chem. Res. 28 (1995) 141–145.
[3] Solar, Wind Technologies for Hydrogen Production: Report to Congress, ESECS EE-3060, U.S. Department of Energy, 2005.
[4] B.D. James, G.N. Baum, J. Perez, K.N. Baum, Technoeconomic analysis of photoelectrochemical hydrogen production, December 2009, DOE Contract Number: GS-10F-009J.
[5] H. Park, Y. Park, W. Kim, W. Choi, J. Photochem. Photobiol. C 15 (2013) 1–20.
[6] H. Park, W. Choi, M.R. Hoffmann, J. Mater. Chem. 18 (2008) 2379–2385.
[7] H. Park, Y.K. Kim, W. Choi, J. Phys. Chem. C 115 (2011) 6141–6148.
[8] J.C. Kim, J. Choi, Y.B. Lee, J.H. Hong, J.I. Lee, J.W. Yang, W.I. Lee, N.H. Hur, Chem. Commun. (2006) 5024–5026.
[9] Y. Tachibana, Interfacial electron transfer reactions in CdS quantum dots sensitized TiO_2 nanocrystalline electrodes, in: L. Vayssieres (Ed.), On Solar Hydrogen & Nanotechnology, Wiley, Singapore, 2009, Chap. 9.
[10] H. Tada, T. Mitsui, T. Kiyonaga, T. Akita, K. Tanaka, Nat. Mater. 5 (2006) 782–786.
[11] D.R. Baker, P.V. Kamat, Adv. Funct. Mater. 19 (2009) 805–811.
[12] J.S. Jang, S.H. Choi, H.G. Kim, J.S. Lee, J. Phys. Chem. C 112 (2008) 17200–17205.
[13] G. Khan, Y.K. Kim, S.K. Choi, H. Park, Bull. Korean Chem. Soc. 34 (2013) 1137–1144.
[14] W. Fan, Q. Lai, Q. Zhang, Y. Wang, J. Phys. Chem. C 115 (2011) 10694–10701.
[15] D. He, L. Yang, S. Kuang, Q. Cai, Electrochem. Commun. 9 (2007) 2467–2472.
[16] Y.K. Kim, H. Park, Energy Environ. Sci. 4 (2011) 685–694.
[17] I. Robel, B.A. Bunker, P.V. Kamat, Adv. Mater. 17 (2005) 2458–2463.
[18] Y.K. Kim, H. Park, Appl. Catal. B 125 (2012) 530–537.
[19] J.M. Haremza, M.A. Hahn, T.D. Krauss, Nano Lett. 2 (2002) 1253–1258.
[20] A.C. Dillon, Chem. Rev. 110 (2010) 6856–6872.
[21] P. Serp, J.L. Figueiredo, Carbon Materials for Catalysis, Wiley, New Jersey, 2009.

[22] H. Park, W. Choi, J. Phys. Chem. B 107 (2003) 3885–3890.
[23] H. Park, W. Choi, J. Phys. Chem. B 108 (2004) 4086–4093.
[24] S. Chen, L.-W. Wang, Chem. Mater. 24 (2012) 3659–3666.
[25] A. Chahboun, A.G. Rolo, S.A. Filonovich, M.J.M. Gomes, Sol. Energy Mater. Sol. Cells 90 (2006) 1413–1419.
[26] K.K. Nanda, S.N. Sarangi, S.N. Sahu, J. Phys. D 32 (1999) 2306–2310.
[27] M. Ichimura, F. Goto, E. Arai, J. Appl. Phys. 85 (1999) 7411–7417.
[28] J.R.L. Fernandez, M. de Souza-Parise, P.C. Morais, Surf. Sci. 601 (2007) 3805–3808.
[29] Y. Park, S.-H. Kang, W. Choi, Phys. Chem. Chem. Phys. 13 (2011) 9425–9431.
[30] J.Y. Roh, Y.H. Kim, C.S. Lee, Curr. Appl. Phys. 11 (2011) S69–S72.
[31] K. Suzuki, M. Yamamoto, M. Kumagai, S. Yanagida, Chem. Lett. 32 (2003) 28–29.
[32] D.S. Ginley, M.A. Butler, J. Electrochem. Soc. 125 (1978) 1968–1974.
[33] A.J. Bard, L.R. Faulkner, Electrochemical Methods: Fundamentals and Applications, 2nd ed, John Wiley & Sons, New York, 2001.
[34] A. Lasia, Hydrogen evolution reaction, in: W. Vielstich, A. Lamm, H.A. Gasteiger (Eds.), Handbook of Fuel Cells, Vol. 2, John Wiley & Sons; West Sussex, 2003.